

Abell 3627: A Nearby, X-ray Bright, and Massive Galaxy Cluster

H. Böhringer, D.M. Neumann, S. Schindler¹

Max-Planck-Institut für extraterrestrische Physik, D-85740 Garching, Germany

R.C. Kraan-Korteweg

Observatoire de Paris, DAEC, Unité associée au CNRS, D0173, et à l'Université Paris 7, 92195 Meudon, France

ABSTRACT

The cluster A3627 was recently recognized to be a very massive, nearby cluster in a galaxy survey close to the galactic plane. We are reporting on ROSAT PSPC observations of this object which confirm that the cluster is indeed very massive. The X-ray emission detected from the cluster extends over almost 1 degree in radius. The X-ray image is not spherically symmetric and shows indications of an ongoing cluster merger. Due to the strong interstellar absorption the spectral analysis and the gas temperature determination are difficult. The data are consistent with an overall gas temperature in the range 5 to 10 keV. There are signs of temperature variations in the merger region.

A mass estimate based on the X-ray data yields values of $0.4 - 2.2 \cdot 10^{15} M_{\odot}$ if extrapolated to the virial radius of $3h_{50}^{-1}$ Mpc. In the ROSAT energy band (0.1 - 2.4 keV) the cluster emission yields a flux of about $2 \cdot 10^{-10} \text{ erg s}^{-1} \text{ cm}^{-2}$ which makes A3627 the 6th brightest cluster in the ROSAT All Sky Survey. The cluster was missed in earlier X-ray surveys because it was confused with a neighbouring X-ray bright, galactic X-ray binary (1H1556-605). The large X-ray flux makes A3627 an important target for future studies.

Subject headings: Galaxies:Clusters of, Cosmology: Large-Scale Structure of Universe, X-rays: Galaxies

1. Introduction

In a deep galaxy survey behind the Milky Way ($|b| \leq 10^\circ$) the cluster A3627 was recently found by Kraan-Korteweg et al. (1996) to be a very rich, nearby cluster of galaxies rivaling the prominent Perseus and Coma clusters in its mass and galaxy content. The observed recession velocity of 4882 km, s⁻¹ corresponding to a velocity of 4655 km s⁻¹ with respect to the Local Group places A3627 at a distance of about 93 Mpc (we are using a Hubble constant of $H_0 = 50 \text{ km s}^{-1} \text{ Mpc}^{-1}$ in this paper). Therefore the cluster is one of the most prominent mass concentrations in the local Universe. Kraan-Korteweg et al. (1996) found a galaxy velocity dispersion of 903 km s⁻¹ and attributed a mass of $5 \cdot 10^{15} M_{\odot}$ to this cluster. Although A3627 has been cataloged by Abell, Corwin & Olowin (1989) as a richness class 1 cluster with 59 galaxies it attracted little attention in the past *because* of its proximity to the galactic plane ($l = 325^\circ$,

¹also at Max-Planck-Institut für Astrophysik, D-85740 Garching, Germany

$b = -7^\circ$). It has also not been detected in previous X-ray surveys (e.g. Piccinotti et al. 1982, Kowalski et al. 1984, Lahav et al. 1989).

We have observed this prominent cluster with the ROSAT PSPC. The results of this observation support the finding of Kraan-Korteweg et al. (1996) that A3627 is a very massive cluster. In this paper we give a detailed report on the X-ray properties of A3627 and describe its structure as revealed by the ROSAT images. Section 2 provides an account of the X-ray morphology. The X-ray spectral analysis is discussed in Section 3. Section 4 describes the mass determination. In Section 5 these results are discussed and Section 6 provides a summary.

2. X-ray Morphology

The cluster A3627 was observed with the ROSAT PSPC in September 1992 and March 1993 for a total exposure time of 11,257 sec. The galactic hydrogen column density at this location is quite high (around $1.8 \cdot 10^{21} \text{ cm}^{-2}$). Therefore no photons are detected in the soft energy band of ROSAT below the carbon edge (0.1 to 0.4 keV). An X-ray image produced from the hard band counts (0.5 - 2 keV) is shown in Fig. 1. The X-ray emission of the cluster fills almost the whole field of view of the detector. The total ROSAT PSPC count rate in the (0.5 to 2.0 keV band) is found to be $7.0 \pm 0.3 \text{ cts s}^{-1}$. The X-ray emission was integrated out to a radius of 51.5 arcmin and the background was taken from the remaining area outside. In addition we also analysed regions inside this radius to the north-east and south-west of the cluster and found that these areas give background values consistent with those from the outer annulus. This comparison shows that uncertainties in the vignetting correction at the very outer edge of the PSPC field do not affect the results. Anyway these uncertainties are expected to be more critical in the soft energy channels and less in the hard part of the ROSAT energy window used here. For a distance of 93 Mpc this corresponds to a flux of $2.1(\pm 0.3) \cdot 10^{-10} \text{ erg s}^{-1} \text{ cm}^{-2}$ and to an X-ray luminosity of $2.2(\pm 0.3) \cdot 10^{44} \text{ erg s}^{-1}$ in the ROSAT energy band (0.1 - 2.4 keV). For these calculations a galactic hydrogen column density of $1.4 - 2.0 \cdot 10^{21} \text{ cm}^{-2}$ and gas temperatures in the range of 5 - 9.5 keV are assumed and the conversion factors are determined using a Raymond-Smith code (Raymond & Smith 1977) with a metallicity of 0.35 in solar units. Furthermore, inspecting the cluster image in the ROSAT All Sky Survey, we find no significant additional X-ray flux beyond a radius of 1 degree. The total cluster count rate in the 0.5 - 2.0 energy band of $6.8 \pm 0.3 \text{ cts s}^{-1}$ determined from the All Sky Survey data is consistent with the result of the pointed observation.

As can be seen in Fig. 1, A3627 is clearly not spherically symmetric. The cluster shows a strong elongation in the direction of PA $\sim 130^\circ$ (measured from north over east). The central maximum of the X-ray emission is at the position 16h14 22, -60d52 20 (J2000) and a secondary X-ray maximum at 16h14 10, -60d50 34. The bright point source about 23 arcmin to the north-west of the cluster center, at the position 16h11 51.7, -60d37 44.0 (J2000), originates from a Seyfert galaxy which was found in the course of the galaxy survey (Woudt et al. 1996). The galaxy was classified as Seyfert 1 and with a velocity of 4711 km s^{-1} it certainly is a cluster member. Another point source, best visible in Fig. 3, is coincident with the radio galaxy PKS1610-60 at the position 16h15 03.7, -60 54 26 (J2000), one of the three central galaxies of the cluster. This source is used to check the attitude of the ROSAT pointing, which is found to be correct within an uncertainty of 3 arcsec. We detect a series of other point sources in the PSPC field of view, that will be described in a follow-up publication.

To see if a varying absorbing hydrogen column density is partly responsible for the observed morphological features, we have studied the hardness variation of the X-ray emission across the cluster image. For this study we mainly use the hardness ratio of the energy bands R4 (PSPC channel 52 - 69) and R5 (PSPC channel 60 - 90). The ROSAT PSPC energy bands are defined by Snowden et al. (1994). These energy bands are closest to the absorption cut-off for the relevant range of column density values and therefore this hardness ratio is sensitive to a variation of the absorbing column density. We do not detect any significant variation of the hardness ratio across the cluster image, however, except that the hardness ratio is much lower for the background than for the cluster.

Assuming that there is an approximately spherically symmetric main component dominating the cluster image, we analyse the surface brightness profile of the western part of the cluster. We use the data from a sector centered on the main maximum (16h14 22, -60d52 20) within the angular region from -180° to 45° (extending from south to north-east in counter-clockwise direction). This region is opposite to the prominent elongation in the cluster and appears therefore less distorted. The surface brightness profile is shown in Fig. 2. We fit a β -model (e.g. Cavaliere & Fusco-Femiano 1976; Jones & Forman 1984) to the surface brightness profile, $S(r)$, (see Fig. 2), using the formula:

$$S(r) = S_0 \left(1 + \frac{r^2}{r_c^2} \right)^{-3\beta+1/2}. \quad (1)$$

Since the core radius of the cluster is so much larger than the resolution of the ROSAT PSPC with a half power radius of 20 arcsec for the point spread function, a convolution with the point spread function does not affect the fitting results significantly and was therefore neglected. The X-ray background is taken as a free fit parameter in this analysis and even though there is not much area at the true background level in the field of view, the fit yields a background value consistent with the one determined from the outermost ring of the PSPC. The resulting fit parameters and their uncertainties are: central surface brightness, $S_0 = 10^{-2}$ counts s⁻¹ arcmin⁻², $\beta = 0.555 (+0.045, -0.035)$, and core radius, $r_c = 9.95 \pm 1.0$ arcmin ($262 \pm 24 h_{50}^{-1}$ kpc). The core radius for the X-ray surface brightness is very similar to the optical core radius of 10.4 arcmin (Kraan-Korteweg et al. 1996). The surface brightness profile keeps increasing inwards inside the core radius and therefore the data points deviate slightly from the β model fit inside a radius of about 5 arcmin. In the outer parts the surface brightness profile is not very smooth. Both deviations from the β model, that generally fits the X-ray surface brightness profile of clusters quite well, may reflect the disturbances by the ongoing merger in the cluster as discussed below.

We use the β model fitted to the less disturbed side of the cluster to construct a synthetic spherically symmetric cluster model that could approximately describe the main body of the cluster. By subtracting this model cluster image from the observed cluster image of Fig. 1, a residual image is obtained (Fig. 3). One can clearly see a very compact cluster component superposed on the main cluster in the south east. This is most likely a smaller subcluster in the process of merging with the main cluster body. The excess X-ray emission is clearly extended and the X-ray spectrum is consistent with a thermal spectrum of hot intracluster plasma (see section 3 and Fig. 6). This characteristics essentially excludes the interpretation of the X-ray emission shown in Fig. 3 as a galactic X-ray source like stars, accretion sources or a supernova remnant.

The morphology displayed in Fig. 3 implies that the merger has obviously already progressed to a stage where the smaller subunit is being distorted. Besides the subcluster there is some excess emission opposite to the subcluster which may reflect details in the dynamics of the merging process.

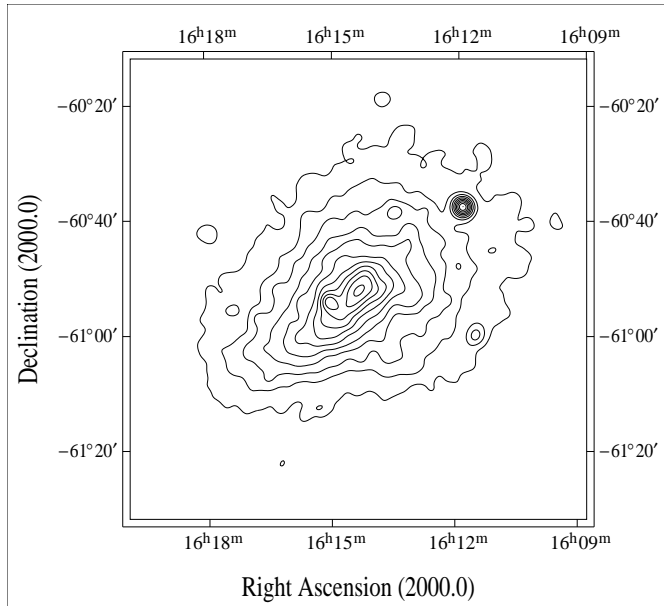


Fig. 1.— ROSAT PSPC image of A3627. Only photons in the hard energy band (0.5 to 2.0 keV) are used and the image is smoothed by a Gaussian with $\sigma = 1$ arcmin. This count rate image is produced from the photon count map by dividing by the exposure map and by correcting for vignetting of the X-ray telescope. The X-ray background was not subtracted. The contour levels start at $1.6 \cdot 10^{-3}$ cts s⁻¹ arcmin⁻² and increase in steps of $9.6 \cdot 10^{-4}$ cts s⁻¹ arcmin⁻².

3. X-ray Spectra

In total about 60,000 photons were received from the cluster X-ray source. This allows us to derive spectra of good statistical quality for different regions in the cluster. Due to the strong absorption in the galactic plane, however, the leverage to constrain the spectral parameters is very small. Therefore it is quite difficult to obtain good constraints for all the spectral parameters simultaneously: temperature, T , hydrogen column density, N_H , and metal abundance. The best strategy to get reliable parameter constraints is to fit the temperature and the absorbing column density simultaneously and to repeat this fitting procedure for the relevant range of expected metallicities. We use metallicity values of 0.2, 0.35 and 0.5 of solar abundances (as quoted by Anders & Grevesse 1989). We find that the metallicity has little influence on the results for T and N_H . For the spectral analysis we remove the four brightest point sources in the cluster.

Fig. 4 shows for example the PSPC spectrum for a large region of the less disturbed part of the cluster. The spectrum is taken from an area in the sector -180° to 90° (excluding the south-eastern quadrant) inside a radius of 10 arcmin. The strong absorption of the soft part of the spectrum is evident. The χ^2 contours for the fit shown in Fig. 5 give the constraints of the temperature and column density and imply an overall cluster temperature in the undisturbed part in the range of 5 to 9.5 keV (for 1σ errors, with best fitting values around 6 - 7 keV). Splitting the area in different subregions does not provide further significant information, since the errors of the measurement are always larger than the differences. However, an indication of a higher temperature in the center prevails. The fits for the central 5 arcmin region show no constraint at the high temperature side and best fitting values around 10 keV.

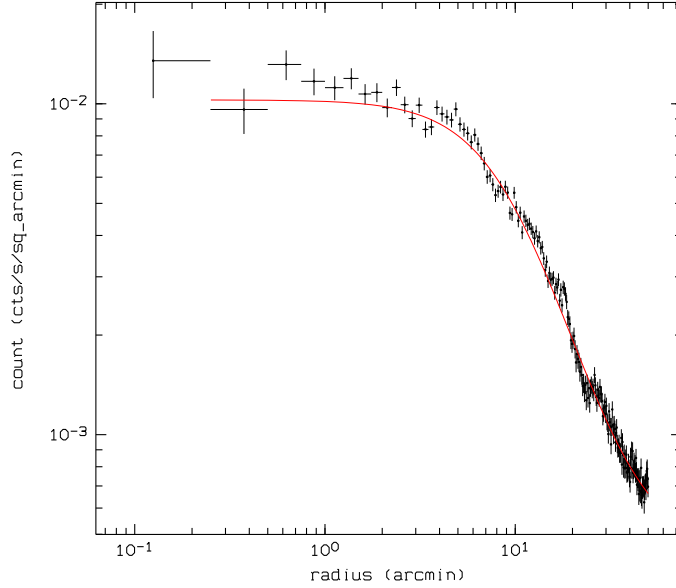


Fig. 2.— X-ray surface brightness profile of A3627 as observed with the ROSAT PSPC. Only photons received in the hard energy band (0.5 - 2 keV) and only data from the region from PA = -180° to PA = 45° were d. The solid line shows the best fitting β model with the parameters $S_0 = 10^{-2}$ cts s $^{-1}$ arcmin $^{-2}$, $\beta = 0.55$, and $r_c = 9.95$ arcmin.

Performing a similar analysis in the disturbed part of the cluster, that is in the sector 90° to 180° (the south-eastern quadrant) we find high temperatures within 5 arcmin of the central region which are of the same order as in the central region of the undisturbed part. In the outer parts of the subclump the temperature is considerably lower ($2.5 \left[_{-0.5}^{+2}\right]$ keV) than in the rest of the cluster. Fig. 6 shows the χ^2 contours for the temperature and column density fit in the subclump for a region with 10 arcmin diameter, centered 13 arcmin south-east of the center. The difference in the temperature of this area and of the overall spectrum has a $\sim 1.5\sigma$ significance. Thus there surely are strong and interesting temperature variations that could provide important information about the merger physics. They should be studied with an X-ray observatory with a wider energy window and a higher spectral resolution, for example ASCA or SAX.

4. Mass Determination

The above results allow to determine the gas mass distribution of the main part of the cluster. We use the fitting results to approximate the gas density profile. For a β model surface brightness profile of the form given in eq.(1), the density of the X-ray emitting plasma is given by

$$\rho_g(r) = \rho_{g0} \left(1 + \frac{r^2}{r_c^2} \right)^{-\frac{3}{2}\beta}, \quad (2)$$

where β is the slope parameter determining the scale height of the gas density distribution. The emissivity of the intracluster plasma is almost independent of the temperature for the energy band covered by the

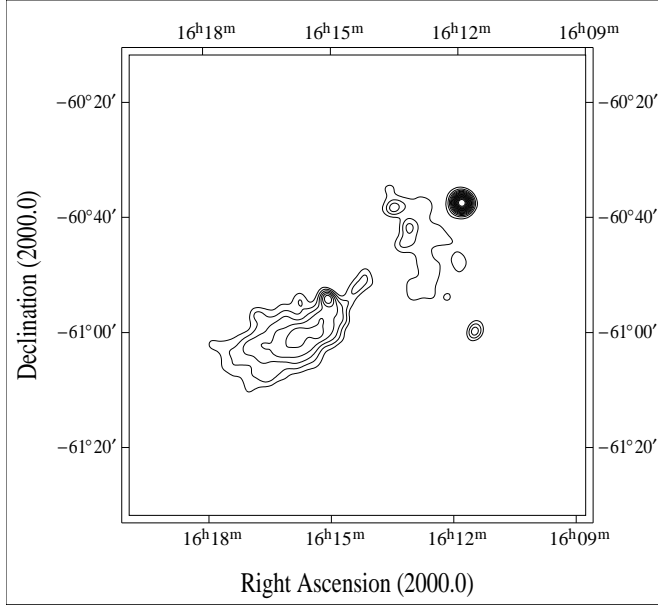


Fig. 3.— Residual X-ray image of A3627 obtained by subtracting a spherically symmetric model from Fig. 1. The parameters for the symmetric model image are taken from a β model fit to the less disturbed side of the cluster as described in the text. The contour levels start at $1.12 \cdot 10^{-3}$ cts $\text{s}^{-1} \text{ arcmin}^{-2}$ and increase in steps of $4.8 \cdot 10^{-4}$ cts $\text{s}^{-1} \text{ arcmin}^{-2}$, so that every second contour corresponds to a contour level in Fig. 1.

ROSAT PSPC. In the temperature range from 2 to 10 keV the emissivity changes only by about 6%. Therefore the imperfect knowledge of the gas temperature introduces only a very small uncertainty in the gas density distribution.

From the gas density distribution and the information on the intracluster temperature we can obtain a gravitational mass estimate of the cluster. We assume that hydrostatic equilibrium of the intracluster gas approximately holds in the main part of the cluster. In fact, Schindler (1996) studied the mass analysis in N-body/hydrodynamic simulations and showed that the assumption of hydrostatic equilibrium leads to very robust results in the mass determination if obvious regions of disturbances are avoided. The gravitational mass of the cluster is determined by

$$M(< r) = -\frac{r kT}{G \mu m_p} \left(\frac{d \log \rho_g}{d \log r} + \frac{d \log T}{d \log r} \right). \quad (3)$$

For the temperature profile we use a range of models: with a given temperature at the core radius between 9.5 and 5 keV, temperature profiles corresponding to polytropic models with values of the polytropic index in the range 0.9 to 1.3 are used. The results for the upper and lower limits to the mass profile are shown in Fig. 7 together with the result for an isothermal model with $T = 7$ keV and the gas mass profile.

The mass profiles in Fig. 7 are extrapolated to a radius of $3h_{50}^{-1}$ Mpc. This should be close to the virial radius of the cluster as explained below. The X-ray emission is only observed to a radius of $1.4h_{50}^{-1}$ Mpc, however. The values for the mass limits for these two radii and for a radius of 1 Mpc are listed in Table 1. The gas mass fractions noted in Table 1 are typical for rich clusters where one finds values in the range 10 - 30% for large radii and sometimes smaller values in the inner regions (e.g. David et al. 1994; Böhringer 1994). The gas mass distribution can be determined quite precisely with the ROSAT data with

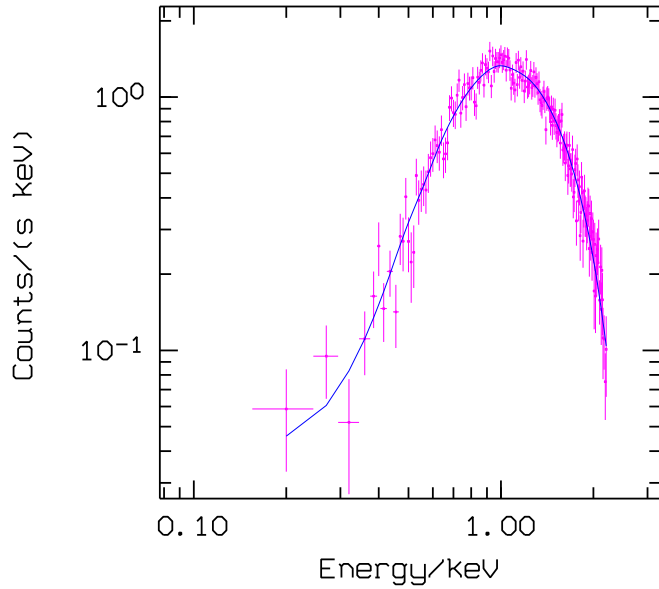


Fig. 4.— X-ray spectrum and fit of a Raymond-Smith model for the less disturbed part of the cluster A3627. The fact that hardly any source photons are received below 0.4 keV is a result of the high absorbing hydrogen column density

little influence from the uncertainty in the temperature. Since the values for the gas mass fractions are consistent with other cluster studies where the spectral data are less affected by absorption, we conclude that the mass estimates are basically correct within the given error limits.

The virial radius of a cluster, r_v , with given mass can be calculated analytically in the limit of the spherical collapse approximation from the formula (see e.g. Gunn & Gott 1972, White et al. 1993):

$$r_v = \left(\frac{M}{1.38 \cdot 10^{15} h_{50}^{-1} M_{\odot}} \right)^{1/2} \Omega^{-0.2} \cdot 3 h_{50}^{-1} \text{ Mpc}. \quad (4)$$

For a closed Universe we find a virial radius of 1.7 – 3.8 Mpc and for $\Omega = 0.4$ values of 2 – 4.5 Mpc. For the most likely isothermal model with $T_g = 7$ keV we obtain $r_v = 2.8 - 3.3$ Mpc for $\Omega = 0.4$ to 1.0, and a total mass $M_v \sim 1.2 \cdot 10^{15} M_{\odot}$ (here the most popular range for the value of Ω is used with a lower bound from the analysis of the large scale velocity fields (e.g. Dekel 1994) and a closed Universe as the upper bound). Therefore one should expect that the virialized part of the cluster system extends to a radius of the order of 3 Mpc.

5. Discussion

In the ROSAT All Sky Survey A3627 is the sixth brightest cluster in the ROSAT band. The brightest clusters in the survey are Virgo, Perseus, Coma, Ophiuchus, and Centaurus with ROSAT PSPC count rates in the 0.5 to 2.0 energy band (channels 52 to 201) of ≥ 80 , 38.3 (± 0.3), 16. (± 0.2), 11.5 (± 0.3), and 9.3

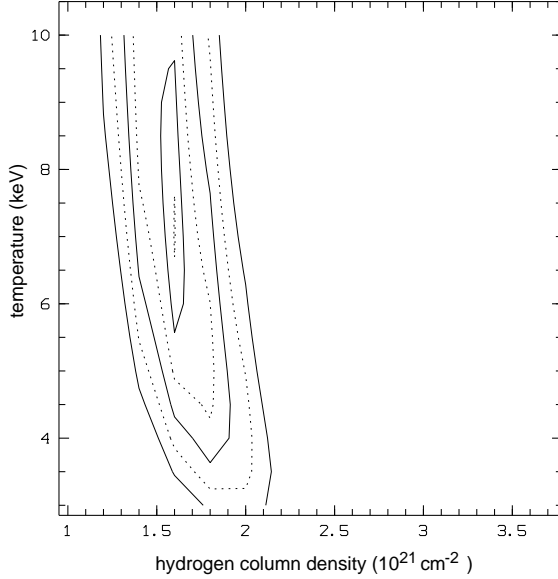


Fig. 5.— χ^2 contours for the fit of a Raymond-Smith model to the X-ray spectrum from the less disturbed part of the cluster out to a radius of 16.7 arcmin. The temperature and the hydrogen column density are varied in the fit. The contour levels encircle the χ^2 minimum and indicate the 1, 2, 3, 4, and 5 sigma levels.

(± 0.2) cts s $^{-1}$, respectively. A3627 follows closely with a ROSAT PSPC count rate of 7.0(± 0.3) cts s $^{-1}$. While the brightest 5 clusters are all very well known and have received a lot of observational attention, e.g. with all recent X-ray observatories, A3627 remained widely unnoticed.

Why has it been overlooked in previous X-ray surveys? For the calculated flux in the ROSAT energy band of $2 (\pm 0.2) \cdot 10^{-10}$ erg s $^{-1}$ cm $^{-2}$, we find an X-ray flux in the 2 - 10 keV energy band of $1.6 - 2.8 \cdot 10^{-10}$ erg s $^{-1}$ cm $^{-2}$. The sensitivity limits of the HEAO 1 survey are, for example, $1.9 \cdot 10^{-11}$ erg s $^{-1}$ cm $^{-2}$ for the A2 instrument (e.g. Jahoda & Mushotzky 1989) and $5 \cdot 10^{-12}$ erg s $^{-1}$ cm $^{-2}$ for the A1 instrument (e.g. Wood et al. 1984). Fig. 8 shows a map of the HEAO 1 - A2 survey with a scale of 20 degrees around the cluster A3627 as obtained from *SKYVIEW* (available on *World Wide Web*). There is indeed a bright X-ray source in the center of the image, labeled as no. 2 (no. 21 in Jahoda & Mushotzky 1989), which is close to the position of the cluster. This source, cataloged as 4U1556-60 or 1H1556-605, is identified with a galactic, low mass X-ray binary (e.g. Motch et al. 1989). The source count rate of 1H1556-605 in the HEAO 1 - A1 survey is 0.0446(± 0.022) cts s $^{-1}$ corresponding to a 2-10 keV flux of about $2 \cdot 10^{-10}$ erg s $^{-1}$ cm $^{-2}$ (Wood et al. 1984).

Fig. 9 shows the region around A3627 in the ROSAT All Sky Survey with a scale of about 4 by 4 degrees. 1H1556-605 is the bright source to the west at a position of 16h 01 02, -60d44 17 (J2000) with a ROSAT PSPC count rate in the hard band (channel 52 - 201) of about 8 cts s $^{-1}$. Thus the flux of the low mass X-ray binary is only slightly higher in the ROSAT band than the integrated X-ray flux from A3627. The fact that the 2 - 10 keV flux expected from A3627 is close to what is observed and that the two sources appear about equally bright in the hard ROSAT band leads to the conclusion that the flux measured for 1H1556-605 in the early X-ray collimator observations contains a significant contribution from the cluster emission. The distance between the two sources is about 1.5 degrees. It is therefore somewhat surprising

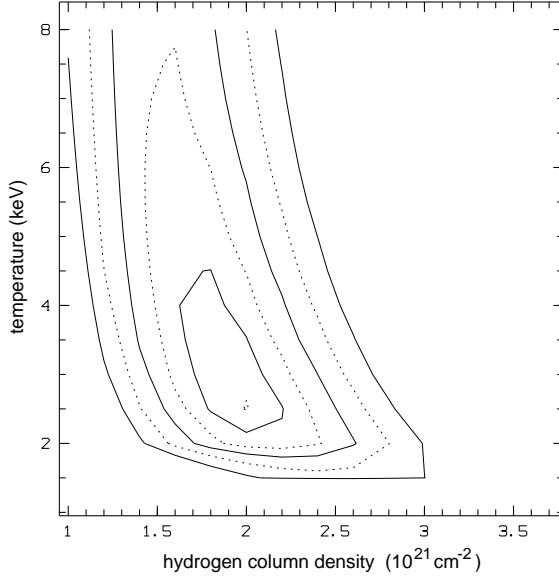


Fig. 6.— χ^2 contours for the fit of a Raymond-Smith model to the X-ray spectrum from a region in the infalling subclump 13 arcmin from the center of A3627. The temperature and the hydrogen column density are varied in the fit. The contour levels encircle the χ^2 minimum and indicate the 1, 2, 3, 4, and 5 sigma levels.

that the X-ray source visible in the HEAO 1 - A2 survey (cf. Fig. 8) is not more distorted compared to the appearance of the other true point sources.

The mass estimate above shows that A3627 has at least half the mass of the Perseus and Coma clusters with masses of $1.0 - 2.6 \cdot 10^{15} h_{50}^{-1} M_{\odot}$ for an outer radius of $3 h_{50}^{-1}$ Mpc (Briel et al. 1991a, Böhringer 1994). It is therefore a very prominent mass concentration in the local Universe. Since it is located in the Great Attractor region it is responsible for part of the gravitational pull causing the local streaming velocity in this direction, as already discussed by Kraan-Korteweg et al. (1996).

The mass obtained from the X-ray study can also be compared to the mass estimate from a virial analysis based on the optical data. For a velocity dispersion of 897 km s^{-1} (corrected for measurement errors), a core radius of $262 h_{50}^{-1} \text{ kpc}$, and an outer radius of $3 h_{50}^{-1}$ Mpc we obtain a mass of $9.5 \cdot 10^{14} h_{50}^{-1} M_{\odot}$ using the formula (e.g. Sarazin 1986):

$$M(< r) = \frac{9\sigma_r^2 r_c}{G} \left(\ln(x + (1 + x^2)^{1/2}) - x(1 + x^2)^{-1/2} \right), \quad (5)$$

where $x = r/r_c$. This result is in very good agreement with the X-ray analysis. It implies that the X-ray temperature estimate is consistent with the optical data.

The mass of A3627 quoted in the paper by Kraan-Korteweg et al. (1996) with a value of $5 \cdot 10^{15} M_{\odot}$ refers to a much larger volume. This mass was obtained by integrating over a galaxy distribution described by a De Vaucouleur profile (e.g. Rood et al. 1972) with effective radius of 155 arcmin ($\sim 4.2 h_{50}^{-1}$ Mpc) with the same galaxy velocity dispersion as used above. This mass therefore corresponds to a larger structure and cannot easily be compared to our mass determination. In addition the mass determined here refers only to the spherically symmetric main part of the cluster.

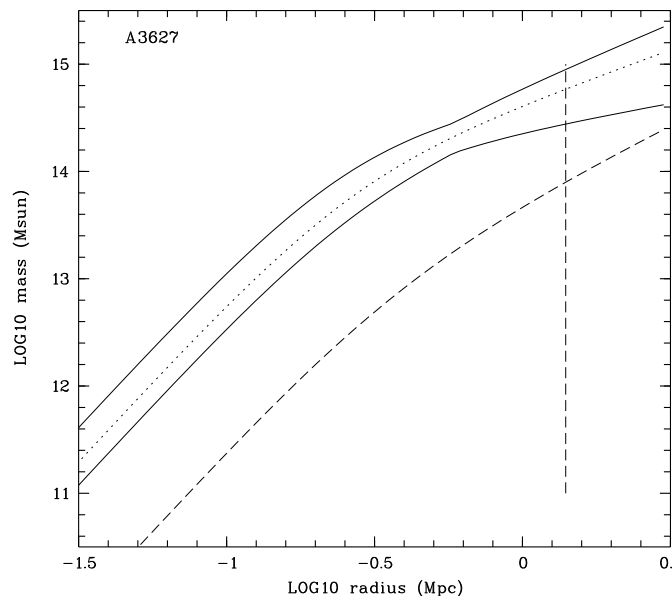


Fig. 7.— Gravitational mass and gas mass profiles of A3627 determined from the X-ray data. The solid curves show the upper and lower limit for the gravitational mass profile calculated for intracluster medium temperatures in the range 5.0 to 9.5 keV. The dotted curve shows the mass profile for an isothermal model with a temperature of 7 keV. The dashed curve gives the gas mass profile determined from the β model fit to the surface brightness profile. The dashed vertical line indicates the outer radius to which X-ray emission from the cluster could be detected. The mass profiles to the right of this line are only extrapolations.

A3627 obviously shows an interesting merger configuration in which a smaller cluster component is merging with the major part in the south-eastern region. The lower temperature found in the south-east indicates that the smaller cluster component had an originally lower gas temperature than the main cluster. This is consistent with the fact that the cluster mass and the gas temperature are generally tightly correlated (e.g. Edge et al.1991, David et al.1993) and that one expects the second component of the cluster to be significantly less massive than the main part from the morphological appearance of the cluster. It also implies that the outer parts of the infalling component have not been heated by the shock waves which are expected from the merger event (e.g. Schindler & Müller 1993).

Two radio galaxies with extended radio lobes found in A3627 may give further insight into the state of the merger. PKS1610-60.8 which appears as a point source in the X-ray image is a wide-angle-tail (WAT) radio galaxy (Christiansen et al. 1977). The radio lobes show an extent of at least 8 arcmin (210 kpc) on both sides with bending angles of about 45° at distances of 1.5 and 4 arcmin from the galactic center. This galaxy, which is located approximately in the middle between the X-ray maxima of the main component and the subcluster, is the the brightest galaxy of the cluster and of elliptical type (see Christiansen et al.1977). The fact that this galaxy is a WAT supports the assumption that it was the central galaxy of the pre-merger main cluster with a small relative velocity with respect to the overall gravitational potential of the cluster. It is somewhat surprising, however, that we don't see a stronger distortion of the radio lobes today, since the galaxy seems to be located in the active region of the present merger.

The other interesting radio galaxy, B1610-60.5 (Jones & McAdam 1994), is located about 14 arcmin

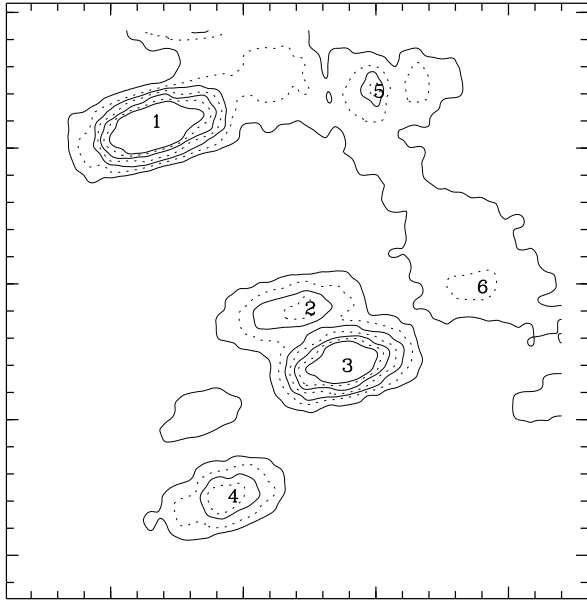


Fig. 8.— X-ray emission from an area of 20 degree diameter around A3627 as observed in the HEAO 1 - A2 All Sky Survey. A3627 is part of the source labeled no. 2. The other sources are of galactic origin and are identified as: 1 = 4U1636-53, 3 = 1H1543-624, 4 = 1H1627-673, 5 = GPS1538-55, and 6 = GPS 1510-58 (see also Jahoda & Mushotzky 1989).

north-east of the X-ray maximum. It is a head-tail radio source and has one of the longest tails ever found with a size of $710h_{50}^{-1}$ kpc (26 arcmin). The tail extends in north-western direction ($PA = 108^\circ$) and stays within an angle of 10° within this direction over the whole length. It is striking that this direction almost coincides with the direction of the line connection the X-ray maxima of the main part and subcomponent of the cluster. The straightness of the tail implies that the intracluster medium was not disturbed by large flows during the passage of the galaxy (for a time of about $7 \cdot 10^8$ years, assuming a galaxy velocity of about 1000 km s^{-1}).

The lack of distortion of the radio lobes of the two radio galaxies and the compactness of the subclump as it appears in Fig. 3 imply that the merger has not progressed very far and that most of the main component of the cluster is still undisturbed by the effects of the collision. Compared to A2256, another famous merging cluster (Briel et al. 1991b), the merging process is closer to completion in A3627. A study of the gas temperature distribution by future X-ray observations and the combination of the present results with the redshift data from the galactic plane galaxy survey will provide a better basis to elucidate the structure of the merging clusters.

6. Summary

The low galactic latitude cluster A3627 ($b = 7^\circ$) which received little attention in the past is the 6th brightest cluster in the sky in the ROSAT energy band. The X-ray flux is high enough that it has even

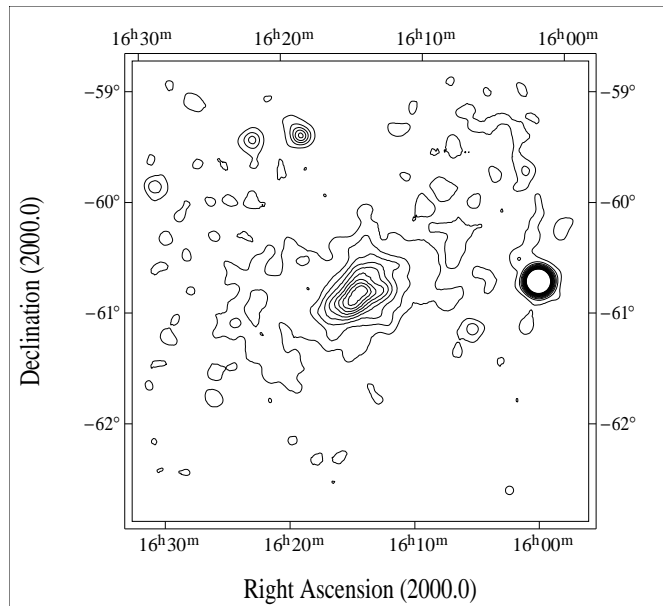


Fig. 9.— X-ray map of the region around A3627 from the ROSAT All Sky Survey. The image is produced from the photons in the 0.5 to 2 keV band. The source in the center is A3627 and the bright point source to the right is the low mass X-ray binary 1H1556-605. Both sources contribute to the HEAO 1 source labeled no. 2 in Fig. 8.

been seen in the Uhuru sky survey but it was confused with a galactic low mass X-ray binary which lies close to it and has a similar X-ray flux.

A3627 has a mass around $10^{15} M_{\odot}$. Therefore it is almost as massive as the prominent Perseus and Coma clusters but, with a redshift of $z = 0.016$, it is even closer. The cluster is an interesting merger system and should be one of the most interesting targets to study cluster mergers with spatially resolved X-ray spectroscopy.

We thank the ROSAT team for providing the ROSAT All Sky Survey data for the area around A3627 and for the excellent performance of the pointed observation on the cluster. We also thank Patrick Woudt for the identification of the X-ray point sources with individual galaxies. H.B. and S.S. are grateful for financial support by the German BMFT through the Verbundforschung for astronomy. S.S. gratefully acknowledges the hospitality of the Astronomical Institute of the University of Basel.

REFERENCES

- Abell, G.O., Corwin, H.G. & Olowin, R.P. 1989, *ApJS*, 70, 1
- Anders, E. & Grevesse, N. 1989, *Geochimica & Cosmochimica Acta*, 53, 197
- Böhringer H. 1994, in *Cosmological Aspects of X-ray Clusters of Galaxies*, NATO ASI Series C Vol. 441, W. C. Seitter (ed.), Kluwer Acad. Publ., Dordrecht, p. 123
- Briel, U.G., Henry, J.P. & Böhringer, H. 1991a, *A&A*, 259, L31

- Briel, U.G., Henry, J.P., Schwarz, R.A., Böhringer, H., Ebeling, H., Edge, A.C., Hartner, G., Schindler, S., Trümper, J. & Voges, W., 1991b, *A&A*, 246, L10
- Cavaliere, A. & Fusco-Femiano, R. 1976, *A&A*, 49, 137
- Christiansen, W.N., Frater, R.H., Watkinson, A., O’Sullivan, J.D., Lockhart, I.A. & Goss, W.M. 1977, *MNRAS*, 181, 183
- David, L.P., Slyz, A., Jones, C., Forman, W., & Vrtillek, S.J., 1993, *ApJ*, 412, 488
- David, L.P., Jones, C., Forman, W., & Daines, S. 1994, *ApJ*, 428, 544
- Dekel, A., 1994 *ARA&A*, 32, 371
- Edge, A.C., & Stewart, G.C., 1991, *MNRAS*, 252, 414
- Gunn, J.E. & Gott, J.R. 1972, *ApJ*, 176, 1
- Jahoda, K. & Mushotzky, R.F. 1989, *ApJ*, 346, 638
- Jones, C. & Forman, W. 1984, *ApJ*, 276, 38
- Jones, P.A. & McAdam, W.B. 1994, *Proc. Astr. Soc. Australia*, 11, 74
- Kowalski, M.P., Ulmer, M.P., Cruddace, R.G. & Wood, K.S. 1984, *ApJS*, 56, 403
- Kraan-Korteweg, R.C., Woudt, P.A., Cayatte, V., Fairall, A.P., Balkowski, C. & Henning, P.A. 1996, *Nat*, (in press)
- Motch, C., Pakull, M.W., Mouchet, M. & Beuermann, K. 1989, *A&A*, 219, 158
- Lahav, O., Edge, A.C., Fabian, A.C. & Putney, A. 1989, *MNRAS*, 238, 881
- Piccinotti, G., Mushotzky, R.F., Boldt, E.A., Holt, S.S., Marshall, F.E., Sermelitsos, P.J. & Shafer, R.A. 1982, *ApJ*, 253, 485
- Raymond, J.C. & Smith, B.W. 1977, *ApJS*, 35, 419
- Rood, H.J., Page, T.L., Kintner, E.C. & King, I.R. 1972, *ApJ*, 175, 627
- Sarazin, C.L. 1986, *Rev. Mod. Phys.*, 58, 1
- Schindler, S., 1996, *A&A*, 305, 756
- Schindler, S. & Müller, E. 1993, *A&A*, 272, 137
- Snowden, S.L., McCammon, D., Burrows, D.N. & Mendenhall, J.A. 1994, *ApJ*, 424, 714
- White, S.D.M., Efstathiou, G. & Frenk, C.S. 1993, *MNRAS*, 262, 1023
- Wood, K.S., Meekins, J.F., Yentis, D.J., Smathers, H.W., McNutt, D.P., Bleach, R.D., Byram, E.T., Chubb, T.A. & Friedman, H. 1984, *ApJS*, 56, 507
- Woudt, P.A., Fairall, A.P., Kraan-Korteweg, R.C. & Cayatte, V. 1996, (in preparation)

Table 1. Gravitational Mass and Gas Mass of A3627

radius ^{a)}	grav. mass ^{b)}	gas mass ^{c)}	gas mass fraction (%)
1.0	2.2 - 5.8	0.46	8 - 21 $h_{50}^{-1.5}$
1.4	2.8 - 9.0	0.8	9 - 29 $h_{50}^{-1.5}$
3.0	4.2 - 22.	2.45	11 - 58 $h_{50}^{-1.5}$

^a radius in h_{50}^{-1} Mpc

^b mass in $h_{50}^{-1} 10^{14} M_{\odot}$

^c mass in $h_{50}^{-2.5} 10^{14} M_{\odot}$